Ijesm
Consulting, help, relaxation
INTERNATIONAL JOURNAL OF ENGINEERING SCIENCES & MANAGEMENT

STARVATION EFFECTS IN ELASTO-HYDRODYNAMICALLY LUBRICATED LINE CONTACTS

PARVEEN KUMAR *
Department of Manufacturing and Automation, India

ABSTRACT

A lubricated contact suffers from starvation when the lubricant does not fill the contact inlet adequately. Such a situation arises due to short lubricant supply or at extremely high speeds. The starvation effect is modeled by shifting the position of the inlet meniscus towards the contact zone. The degree of starvation, so obtained, is plotted as a function of the position of inlet meniscus under different operating conditions. Various degrees of starvation are obtained by shifting the inlet meniscus from its fully flooded position toward the Hertzian contact zone. In this work, the effect of starvation on the two most important parameters necessary for EHL performance evaluation which are coefficient of friction and central film thickness has been studied at different loads and rolling speeds.

Keyword: Elasto-hydrodynamic lubrication, Film thickness, Coefficient of friction, Starvation, line contacts.

INTRODUCTION

Lubrication involves the separation of the surfaces pressed against each other under load, and in relative motion by introducing a layer of fluid between them. In the case of hydrodynamic lubrication a fluid film is produced between the contacting surfaces and the pressure generated in the film balances the applied load. The study of the hydrodynamic lubrication by taking account of elastic deformation of the contacting surfaces and piezo-viscous increase in lubricant viscosity is known as elastohydrodynamic lubrication.

Within the field of elastohydrodynamic lubrication, two main geometrical arrangements can be distinguished. In the first arrangement, two cylinders may represent elements with parallel axes, which contact along a common generator. This configuration is termed as line contact and is typical of cylindrical rolling element bearings, spur gears and cams. A second type of contact occurs where the lubricated elements touch at a single point. In this case, cylinders may represent bearing elements with their axes crossed or by the contact between a sphere and a plane surface. This arrangement is called point contact and occurs in spherical rolling element bearings. The success of the lubrication system depends upon the existence of a fluid film, which has a thickness on the order of a few hundred nanometers or even less. Therefore, it is important to be able to predict the fluid film thickness along with the other associated parameters such as pressure distribution, coefficient of friction under a given set of operating conditions at the design stage. In order to meet the growing demand of industry for highly advanced technologies, the operating loads are increasing, the fluid films are becoming thinner and special purpose lubricants are being employed. Moreover, due to increasing competition in the global market, the emphasis is on lower costs and longer lives of the components. In view of these facts, it is necessary to develop a better understanding of EHL as well as to update and simplify the existing methods for analyzing the problems of elastohydrodynamic lubrication.

Due to the aforesaid reasons, the focus of attention has shifted to more realistic and complex situations. The detailed survey of literature, presented in

***Corresponding Author**
parveenkumar1606@gmail.com

Chapter 2, reveals that a lot of work has been carried out over the last few decades in order to replace the conventional elastohydrodynamic lubrication theory by more realistic approach involving several physical effects. Despite these efforts, a major aspect of practical EHL behavior still remains largely unexplored. This includes the effect of starvation in EHL contacts. Hence, a numerical investigation is performed in the present work for a Newtonian fluid to analyze the influence of starvation in elastohydrodynamic lubrication of line contacts. Starvation refers to the inadequate filling of the conjunction and it is modeled by shifting the inlet meniscus towards the contact zone. The Reynolds equation, which governs the generation of pressure in the lubricated contact, is discretized using finite differences and solved along with the load balance equation using Newton-Raphson technique.

Numerical Model: The analysis of isothermal elastohydrodynamic lubrication of line contacts, as shown in Fig involves the simultaneous solution of Reynolds equation, elasticity equation and load equilibrium equation subject to appropriate boundary conditions with due consideration to the variation of the fluid properties - viscosity and density, with pressure. Therefore, the following subsections present a detailed description of the governing equations.

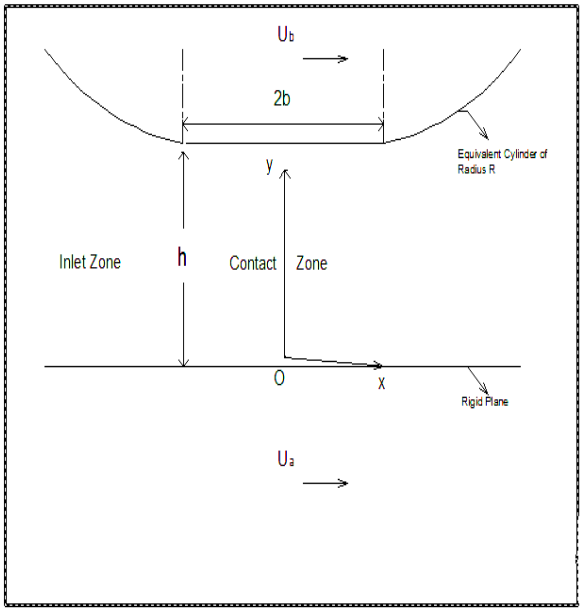

Fig Contact geometry and co-ordinate axes

Reynolds Equation: The classical Reynolds equation is given below in dimensionless form:

$$\frac{\partial}{\partial X}\left(\frac{\bar{\rho}H^{3}\partial P/\partial X}{\bar{\eta}}\right)-K\frac{\partial}{\partial X}(\bar{\rho}H)=0$$

$$K=\frac{3U\pi^{2}}{4W^{2}}$$

Where,

Finite Difference Formulation: The Reynolds equation is discretized by using a finite differencing scheme to obtain the equations $f_i = 0$ (2 to N) as follows:

$$f_i=\varepsilon_{i+1/2}\frac{P_{i+1}-p_i}{\Delta X^{2}}-\varepsilon_{i-1/2}\frac{P_i-p_{i-1}}{\Delta X^{2}}-K\frac{\left[(\bar{\rho}H)_i-(\bar{\rho}H)_{i-1}\right]}{\Delta X}$$

Where, $\varepsilon_i=\left(\frac{\bar{\rho}H^{3}}{\bar{\eta}\xi}\right)_i$

NEWTON-RAPHSON FORMULATION

The simultaneous system of *N* equations by discretized Reynolds equation (3. 4) and discretized load equilibrium equation (3.19) are solved using the Newton-Raphson technique. The N system unknowns are $P_2, P_3, P_4, ..., P_N$ and H_0. The matrix equation of this system is

$$\begin{bmatrix} \frac{\partial f_2}{\partial P_2} & \frac{\partial f_2}{\partial P_3} & \cdots & \frac{\partial f_2}{\partial P_N} & \frac{\partial f_2}{\partial H_0} \\ \frac{\partial f_3}{\partial P_2} & \frac{\partial f_3}{\partial P_3} & \cdots & \frac{\partial f_3}{\partial P_N} & \frac{\partial f_3}{\partial H_0} \\ \cdots & \cdots & \cdots & \cdots & \cdots \\ \vdots & \vdots & \vdots & \vdots & \vdots \\ \frac{\partial f_N}{\partial P_2} & \frac{\partial f_N}{\partial P_3} & \cdots & \frac{\partial f_N}{\partial P_N} & \frac{\partial f_N}{\partial H_0} \\ C_2 & C_3 & \cdots & C_N & 0 \end{bmatrix} \begin{bmatrix} \Delta P_2 \\ \Delta P_3 \\ \cdots \\ \cdots \\ \Delta P_N \\ \Delta H_0 \end{bmatrix} = - \begin{bmatrix} f_2 \\ f_3 \\ \cdots \\ \cdots \\ f_N \\ \Delta W_0 \end{bmatrix}$$

The elements of the Jacobian matrix $[J]$ are calculated as described in Appendix 1.

Degree of starvation

The degree of starvation (σ) is defined as the fractional loss in the weighted mass flow rate:

$$\sigma = 1 - \frac{\left\{\rho h_c u_o \left[KH - \frac{H^3}{\bar{\eta}}\frac{\partial P}{\partial X}\right]\right\}_{Starved}}{\left\{\rho h_c u_o \left[KH - \frac{H^3}{\bar{\eta}}\frac{\partial P}{\partial X}\right]\right\}_{Fully-flooded}}$$

COEFFICIENT OF FRICTION

The pressure distribution and film shape obtained by solving the governing equation are used the determine of the coefficient of friction. The coefficient of friction (μ) is taken as the ratio of total shear force of the lubricant at the surface boundaries and the applied normal load as expressed by the following equation

$$\mu = \frac{\int_{x_i}^{x_o} \tau(y=0)dx}{w}$$

The corresponding non- dimensional form is:

$$\mu = \sqrt{\frac{8}{\pi W}} \int_{X_{ini}}^{X_o} \left(\frac{\pi S U \bar{\eta}}{8WH} - \frac{WH}{\pi}\frac{dP}{dX}\right) dX$$

Solution Procedure:

The steps involved in the overall solution scheme are given below:

1. The pressure distribution[*P*], offset film thickness H_o and outlet boundary co-ordinate X_o are initialized to some reference values.
2. The current pressure distribution is used to calculate surface displacements $[\bar{v}]$ using elasticity equation.
3. The surface displacements $[\bar{v}]$ are used along with the offset film thickness H_o to evaluate the fluid film thickness, *H*, at every node by using film thickness equation.
4. The fluid density and viscosity are updated as per the current values of pressure by using equations.
5. The residual vector [*f*] is calculated from the equation of finite difference formulation.
6. The residual vector Δ*W* is calculated from the discretized load equilibrium equation.
7. The residual vectors calculated in the steps 6 and 7 are assembled in a single vector [*F*] to facilitate execution of Newton-Raphson scheme.
8. This is followed by computation of Jacobian coefficients, as described in Appendix-1, to get the Jacobian matrix [*J*].
9. The corrections to the system variables, specified by vectors on the left hand side of equation of newton-raphson formulation are computed by inverting the Jacobian matrix using Gauss elimination.
10. The corrections, calculated in step 9, are added to the corresponding system variables to get the new values of the pressure distribution [*P*] and offset film thickness H_o.
11. The outlet boundary co-ordinate X_o is corrected by using equations of boundary conditions.
12. The X-coordinate of the node nearest to the outlet boundary is set equal to X_N such that $X_N < X_o$. This decides the number of nodes *N* in the solution domain.
13. The pressure gradients along the fluid film are calculated.
14. The convergence criteria given by equations

$$\frac{\left|\left[\sum_{i=1}^{N} P_i\right]_n - \left[\sum_{i=1}^{N} P_i\right]_{n-1}\right|}{\left|\left[\sum_{i=1}^{N} P_i\right]_{n-1}\right|} \le TOL$$

$$\frac{\left|[H_o]_n - [H_0]_{n-1}\right|}{\left|H_o\right|_{n-1}} \le TOL$$

are checked. If any one or more of the relevant criteria are not satisfied, the next iteration begins and the control is shifted back to the step 2.

Starved EHL Characteristics: The starvation effect in EHL line contacts is modeled by shifting the position of the inlet meniscus towards the contact zone. The degree of starvation, so obtained, is

plotted as a function of the position of inlet meniscus under different operating conditions. The following subsections also describe the effect of starvation on the two most important parameters necessary for EHL performance evaluation – coefficient of friction and central film thickness – at different loads, rolling speeds, contact geometries and piezo-viscous coefficients of lubricant.

Effect of LOAD: Figure 1 compares the variation of the degree of starvation (σ) with the position of inlet meniscus (X_{in}) for three different values of maximum Hertz pressure (p_H=0.5, 1 and 2GPa) while the rolling velocity is kept constant at u_o=0.1 m/s. As apparent from Fig. 1 X_{in} = -6 corresponds to σ = 0 and hence, fully flooded condition, whereas, X_{in} = -1 marks the beginning of the contact zone. It can be seen from Fig. 1 that σ increases gradually with an initial shift in the inlet meniscus towards the contact zone. As the inlet meniscus approaches closer to X_{in} = -1, an abrupt increase in the degree of starvation is observed. However, this steep increase in the degree of starvation is noticed much later at p_H=2 GPa than at p_H =0.5 GPa. This is consistent with the well-known fact that the pressure distribution in an EHL contact approaches the Hertzian distribution at high loads, which implies that the pressure build-up starts quite close to the beginning of contact zone and hence, the inlet zone shrinks significantly. This observation is useful while selecting the inlet boundary for fully flooded condition at a given load.

Figure 2 compares the pressure distributions and film profiles for two different positions of the inlet meniscus (X_{in} = -6 and -1.05) at p_H=0.5GPa and u_o=0.1 m/s. It can be seen that even though an appreciable amount of pressure is generated within the inlet for X_{in}=-6, the contact zone pressures differ only marginally for the two positions of inlet meniscus considered here. However, the film profiles clearly show the effect of starvation as the film at X_{in}=-1.05 is much thinner than that at X_{in}= -6. This film-thinning is the most serious consequence of inadequate filing of the EHL conjunction as it may lead to film failure leading to metal-metal contact and hence, increased friction and wear. Further, in order to study the effect of load, Fig. 3 shows the same characteristics as in Fig. 2 at a much higher load, i.e., p_H=2GPa keeping the other parameters same. It is quite apparent that pressure within the inlet zone reaches a negligibly small value unlike the case of p_H=0.5 GPa (Fig. 2). Also, the film profiles at the two inlet meniscus positions indicate a much less pronounced starvation effect. As mentioned above, starvation causes an increase in the value of coefficient of friction (COF). This effect may be quantified in terms of the ratio of COF values obtained under starved and fully flooded conditions. The variation of this ratio with the degree of starvation is compared at p_H=1 and 2 GPa with u_o fixed at 0.1 m/s. It can be seen that coefficient of friction increases by factors exceeding 2, which is quite high. Also, it is apparent that at higher load, the maximum increase in COF is higher. The reason for this increase in coefficient of friction due to starvation can be understood by considering the factors on which it depends, i.e., contact zone viscosity and shear rate. The contact zone viscosity remains almost unaffected as it is observed that pressure does not undergo any noticeable change. The shear rate, however, increases due to the film-thinning caused by starvation. This increase in the shear rate results in higher shear stresses and hence, higher coefficient of friction.

Figure 5 shows the variation of central film thickness with the degree of starvation at p_H= 0.5, 1 and 2 GPa. The slope of the curve increases with decreasing load. Under fully flooded condition, σ = 0, the difference between the central film thickness values at the three loads is maximum. This gap decreases with increasing degree of starvation and the central film thickness tends to converge to a common value independent of the load.

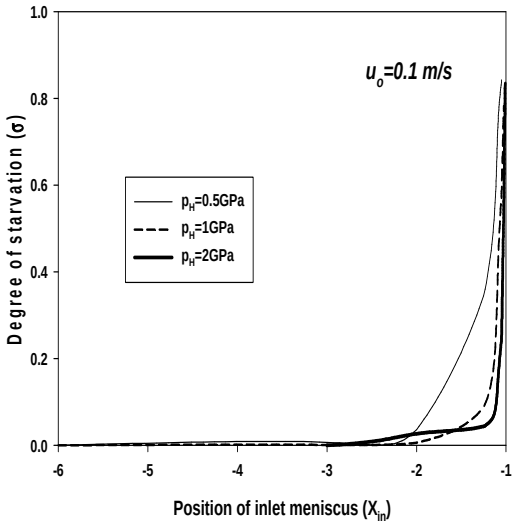

Fig. 1 Variation of the degree of starvation with the position of the inlet meniscus for different Hertzian pressures at u_o=0.1 m/s, α=20 GPa^{-1} and R=0.02 m

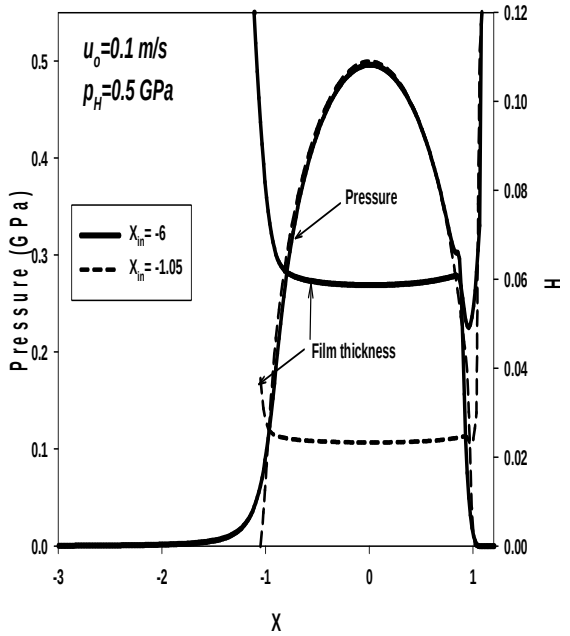

Fig. 2 Comparison of pressure distributions and film shapes at two different positions of inlet meniscus for p_H=0.5 GPa, u_o=0.1 m/s, α=20 GPa^{-1} and R=0.02 m

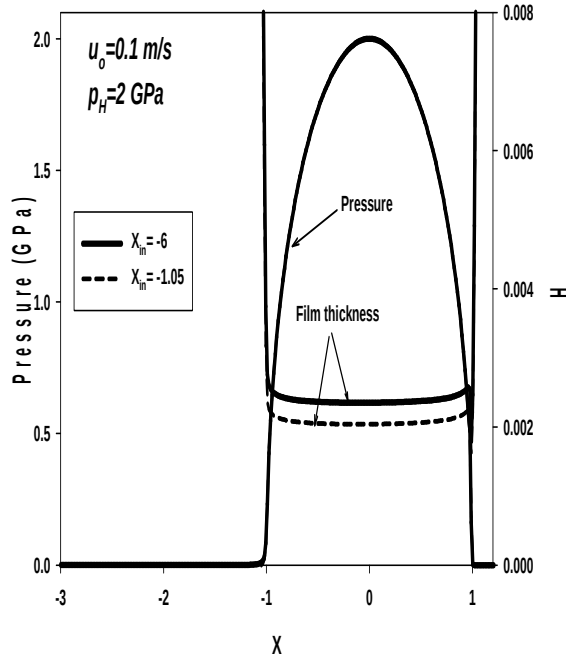

Fig. 3 Comparison of pressure distributions and film shapes at two different positions of inlet meniscus for p_H=2 GPa, u_o=0.1 m/s, α=20 GPa^{-1} and R=0.02 m

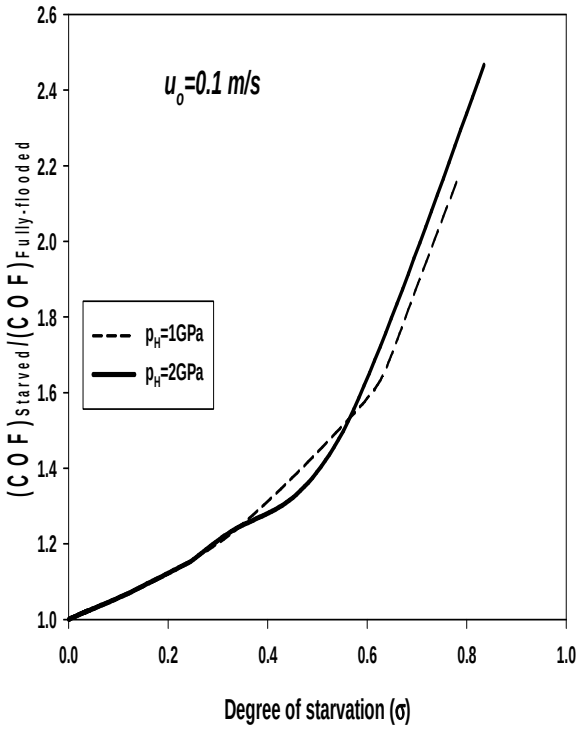

Fig. 4 Variation of the factor by which the coefficient of friction increases with the degree of starvation for different Hertzian pressures at u_o=0.1 m/s, α=20 GPa^{-1} and R=0.02 m

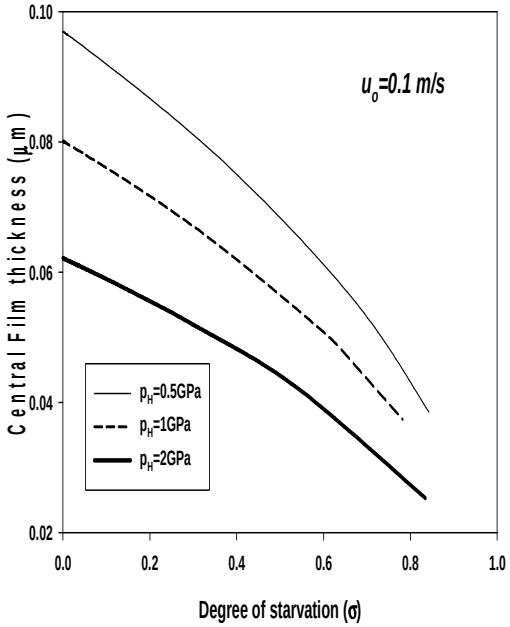

Fig. 5 Variation of central film thickness with the degree of starvation for different Hertzian pressures at u_o=0.1 m/s, α=20 GPa^{-1} and R=0.02 m

CONCLUSION

A lubricated contact suffers from starvation when the lubricant does not fill the contact inlet adequately. Such a situation arises due to short lubricant supply or at extremely high speeds. A detailed study of the influence of various operating parameters on starvation effects in EHL line contacts has been presented in the previous chapter. The starvation effect is modeled by shifting the position of the inlet meniscus towards the contact zone. The degree of starvation, so obtained, is plotted as a function of the position of inlet meniscus under different operating conditions. The effect of starvation on the two most important parameters necessary for EHL performance evaluation – coefficient of friction and central film thickness – has been studied at different loads, rolling speeds, contact geometries and piezo-viscous coefficients of lubricant. Some of the salient conclusions are outlined below:

1. At higher load, the maximum increase in COF is higher. The reason for this increase in COF is the increased shear rates due to the film-thinning attributed to starvation. This increase in the shear rate results in higher shear stresses and hence, higher coefficient of friction.
2. Degree of starvation and the central film thickness tends to converge to a common value independent of the load.
3. The difference in contact zone pressures under fully-flooded and starved conditions is negligible at larfer radius of curvature, whereas, a slight increase is noticeable at smaller radius.
4. Starvation effect on EHL characteristics diminishes with increasing radius for a given location of inlet meniscus.

FUTURE WORK

It would be quite worthwhile to include thermal effect in starvation analysis as the lubricant viscosity undergoes a substantial reduction due to temperature rise. Also, a quantitative validation of simulation results by experimental findings is a great challenge for future.

APPENDIX - 1

DERIVATIVES FOR JACOBIAN MATRIX IN NEWTON-RAPHSON FORMULATION

The derivatives of the residues, f_i, of the finite difference Reynolds equation constituting the Jacobian matrix $[J]$, as given in newton-raphson formulation, are calculated as follows:

$$\frac{\partial f_i}{\partial H_0} = \frac{1}{2}\left(\frac{\partial \varepsilon_{i+1}}{\partial H_0} + \frac{\partial \varepsilon_i}{\partial H_0}\right)\frac{P_{i+1} - P_i}{\Delta X^2} - \frac{1}{2}\left(\frac{\partial \varepsilon_{i-1}}{\partial H_0} + \frac{\partial \varepsilon_i}{\partial H_0}\right)\frac{P_i - P_{i-1}}{\Delta X^2} - K\frac{\left(\bar{\rho}_i - \bar{\rho}_{i-1}\right)}{\Delta X}$$

where,

$$\frac{\partial \varepsilon_i}{\partial H_0} = \frac{\bar{\rho}_i}{\bar{\eta}_i}\left(3H_i^{\,2}\right)$$

$$k_{i-1,j} = \begin{cases} 0 & i-1 \neq j \\ 1 & i-1 = j \end{cases}, \quad k_{i,j} = \begin{cases} 0 & i \neq j \\ 1 & i = j \end{cases}, \quad k_{i+1,j} = \begin{cases} 0 & i+1 \neq j \\ 1 & i+1 = j \end{cases}$$

$$\frac{\partial \varepsilon_i}{\partial P_j} = \frac{\bar{\rho}_i}{\bar{\eta}_i}\left(3H_i^{\,2}\partial H_i / \partial P_j\right) + H_i^{\,3}\left(\frac{\bar{\eta}_i \partial \bar{\rho}_i / \partial P_j - \bar{\rho}_i \partial \bar{\eta}_i / \partial P_j}{\bar{\eta}_i^{\,2}}\right)$$

$$\frac{\partial \overline{\eta}_i}{\partial P_j} = 5.1\times10^{-9} k_{ij} p_h \overline{\eta}_i z \left(\ln \eta_o + 9.67\right)\left(1+5.1\times10^{-9} P p_h\right)^{z-1}$$

$$\frac{\partial \overline{\rho}_i}{\partial P_j} = \frac{0.6\times10^{-9} k_{ij} p_h}{\left(1+1.7\times10^{-9} P_i p_h\right)^2}\left(1-\beta\left(\overline{\theta}_{m,i}-1\right)\theta_o\right)$$